



Direct evidence from anisotropy of magnetic susceptibility for lateral melt migration at superfast spreading centers

Robert J. Varga

Department of Geology, Whitman College, Walla Walla, Washington 99362, USA (vargarj@whitman.edu)

Andrew J. Horst

Department of Earth Sciences, Syracuse University, Syracuse, New York 13244, USA

Jeffrey S. Gee

Geosciences Research Division, Scripps Institution of Oceanography, La Jolla, California 92093-0220, USA

Jeffrey A. Karson

Department of Earth Sciences, Syracuse University, Syracuse, New York 13244, USA

[1] Rare, fault-bounded escarpments expose natural cross sections of ocean crust in several areas and provide an unparalleled opportunity to study the end products of tectonic and magmatic processes that operated at depth beneath oceanic spreading centers. We mapped the geologic structure of ocean crust produced at the East Pacific Rise (EPR) and now exposed along steep cliffs of the Pito Deep Rift near the northern edge of the Easter microplate. The upper oceanic crust in this area is typified by basaltic lavas underlain by a sheeted dike complex comprising northeast striking, moderately to steeply southeast dipping dikes. Paleomagnetic remanence of oriented blocks of dikes collected with both Alvin and Jason II indicate clockwise rotation of $\sim 61^\circ$ related to rotation of the microplate indicating structural coupling between the microplate and crust of the Nazca Plate to the north. The consistent southeast dip of dikes formed as the result of tilting at the EPR shortly after their injection. Anisotropy of magnetic susceptibility of dikes provides well-defined magmatic flow directions that are dominantly dike-parallel and shallowly plunging. Corrected to their original EPR orientation, magma flow is interpreted as near-horizontal and parallel to the ridge axis. These data provide the first direct evidence from sheeted dikes in ocean crust for along-axis magma transport. These results also suggest that lateral transport in dikes is important even at fast spreading ridges where a laterally continuous subaxial magma chamber is present.

Components: 2965 words, 5 figures.

Keywords: spreading centers; magma migration; anisotropy of magnetic susceptibility; East Pacific Rise; Easter microplate.

Index Terms: 3035 Marine Geology and Geophysics: Midocean ridge processes; 3618 Mineralogy and Petrology: Magma chamber processes (1036); 3614 Mineralogy and Petrology: Mid-oceanic ridge processes (1032, 8416).

Received 27 April 2008; **Revised** 2 June 2008; **Accepted** 11 June 2008; **Published** 16 August 2008.

Varga, R. J., A. J. Horst, J. S. Gee, and J. A. Karson (2008), Direct evidence from anisotropy of magnetic susceptibility for lateral melt migration at superfast spreading centers, *Geochem. Geophys. Geosyst.*, 9, Q08008, doi:10.1029/2008GC002075.

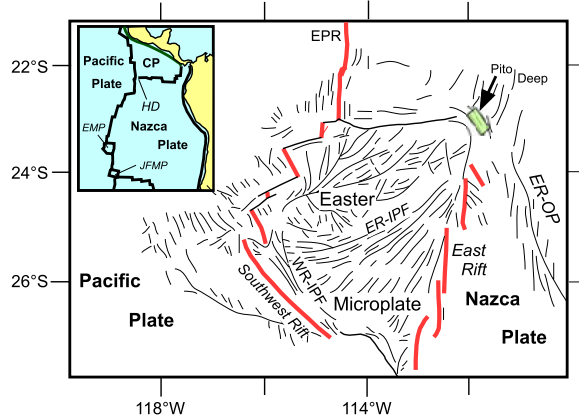


Figure 1. Location and tectonic setting of the Easter microplate (EMP) and the Pito Deep Rift areas of the southern East Pacific Rise (EPR). Fine lines are bathymetric lineaments and are presumed to be parallel to fissures and faults. Thick lines are segments of the EPR surrounding the EMP. CP, Cocos plate; HD, Hess Deep Rift; JFMP, Juan Fernandez microplate; WR-IPF, western ridge inner pseudofault; ER-IPF, eastern ridge inner pseudofault; ER-OP, eastern ridge outer pseudofault. Modified from *Searle et al.* [1989] with permission from Macmillan Publishers Ltd.

[2] Increments of plate separation at oceanic spreading centers are accommodated, in part, by dike intrusion. At relatively high spreading rates (>50 mm/a), virtually continuous magma chambers beneath spreading centers feed magma through dikes, in some cases resulting in surface eruptions of basaltic lavas [*Cann, 1970*]. In detail, oceanic spreading centers appear to be both structurally and magmatically segmented with magmatic activity focused near segment centers and less robust toward segment extremities [*Dunn and Toomey, 1997; Macdonald et al., 1988; White et al., 2000*]. Although it has been suggested on the basis of studies of exposed and eroded ocean crustal analogs [*Baragar et al., 1987; Sigurdsson and Sparks, 1978; Staudigel et al., 1999; Varga et al., 1998*], there is little direct evidence for lateral transport of magma from modern spreading centers. Probable diking events along spreading centers have been inferred in a number of localities, coupled in some cases by corresponding seismic events interpreted as indicating lateral magma flow through a dike [*Delaney et al., 1998*]. Our study complements these indirect observations with direct evidence for lateral magma migration from the dikes themselves. We present anisotropy of magnetic susceptibility (AMS) results for sheeted dikes collected and oriented in situ from remarkable, mid-crustal cliff face exposures of the Pito Deep Rift in the

southern Pacific Ocean. AMS fabric, widely shown to be a reliable proxy for magma transport structure in igneous rocks [*Knight and Walker, 1988; Macdonald and Palmer, 1990; Varga et al., 1998*], offers direct insights into magma flow in crust formed at the superfast spreading East Pacific Rise (EPR). Our results demonstrate the importance of lateral magma flow, even at superfast spreading ridges which typically show evidence for nearly continuous magma chambers. Not only is this study the first to directly demonstrate lateral flow of mid-crustal magmas, it is the first to use AMS on *fully* oriented rocks from the oceans demonstrating the utility of this approach to study of magmatic processes in oceanic crust.

[3] Located at $\sim 23^\circ\text{S}$, the Pito Deep Rift (Figure 1) is a $>6,000$ m-deep, elongate extensional basin with flanking, fault-bounded cliff faces exposing more than 4,000 m of upper and middle crustal rocks. The Pito Deep Rift is one of several rifted areas in the ocean floor where steep, fault-bounded escarpments expose nearly complete vertical sections of the ocean crust. These so-called “tectonic windows” offer a unique three-dimensional view of the detailed architecture of ocean crust not available at actively spreading ridges [*Karson, 1998*] or by deep crustal drilling. Rock units exposed at the Pito Deep Rift include basalt lava (principally pillowed) in the upper part of the section, sheeted dikes and gabbro. In this study we focus on the sheeted dike complex which crops out beneath approximately 600 m of basaltic lavas. These rock units were originally formed ~ 3 Ma along the superfast spreading (full spreading rate > 140 mm/a.) Southern East Pacific Rise. The Pito Deep Rift cut into this crust about 1 Ma as the amagmatic tip of a propagating segment of the East Pacific Rise advanced northward. The Rift forms the eastern boundary of the Easter microplate which appears to be moving independently with respect to the Nazca Plate to the north and has rotated on average clockwise $\sim 21^\circ/\text{Ma}$ over the past ~ 5 Ma [*Naar and Hey, 1991*]. Both magnetic anomaly boundaries and bathymetric lineaments in the area northeast of the Pito Deep Rift and outside of the microplate (Figure 2) are rotated $\sim 20\text{--}45^\circ$ clockwise with respect to $\sim \text{N/S}$ oriented fabrics of the East Pacific Rise [*Karson et al., 2005; Martinez et al., 1991; Rusby and Searle, 1995*] indicating coupling between the microplate and outlying Nazca crust. The northwest trending fault scarps flanking the Pito Deep Rift cut the rotated, northeast trending fabric resulting in the observed,



nearly cross-sectional views of the upper to middle crust.

[4] Our 2005 cruise to the Pito Deep Rift [Karson *et al.*, 2005] was motivated by earlier studies [Francheteau *et al.*, 1994] that demonstrated the presence of well-exposed regions of crustal as well as mantle rocks along several southwest facing fault escarpments. These earlier results helped us identify two promising areas for further detailed study (Figure 2). In addition to detailed SeaBeam and sea-surface magnetometer mapping of the area surrounding the Pito Deep Rift, we mapped the fine detail of the two study areas using DSL-120 side-scan sonar which helped focus a series of subsequent transects using the remotely operated vehicle (ROV) Jason II and the submersible Alvin [Karson *et al.*, 2005]. During this dive program we collected oriented blocks of sheeted dike rock and gabbro using the Geocompass [Hurst *et al.*, 1994] from the steep canyon walls of the Pito Deep Rift. This device allowed us to fully characterize the orientation of several surfaces on each block enabling the blocks, and subsequent cores cut from them, to be later reoriented. Our suite of oriented samples was collected from 15 separate dives in both focus areas (“A” and “B” in Figure 2). A +14° correction was added to all Geocompass measurements based on empirical comparison of gyroscopic and magnetic north directions on sev-

eral control dives. This correction is close to the expected magnetic declination in the area suggesting little vehicle (Jason II or Alvin) related interference. Multiple standard paleomagnetic cores were drilled from each reoriented block. In this study we present AMS and accompanying magnetic remanence results from 36 blocks of sheeted dike rock collected during both Alvin and Jason II dives. While several previous studies have presented paleomagnetic results from oriented samples collected using Alvin [Cogné *et al.*, 1995; Hurst *et al.*, 1994; Varga *et al.*, 2004] or vertical drilling [Allerton and Tivey, 2001], our study is the first to report AMS on ocean rocks from *fully* oriented samples as well as the first to collect oriented block samples using an ROV.

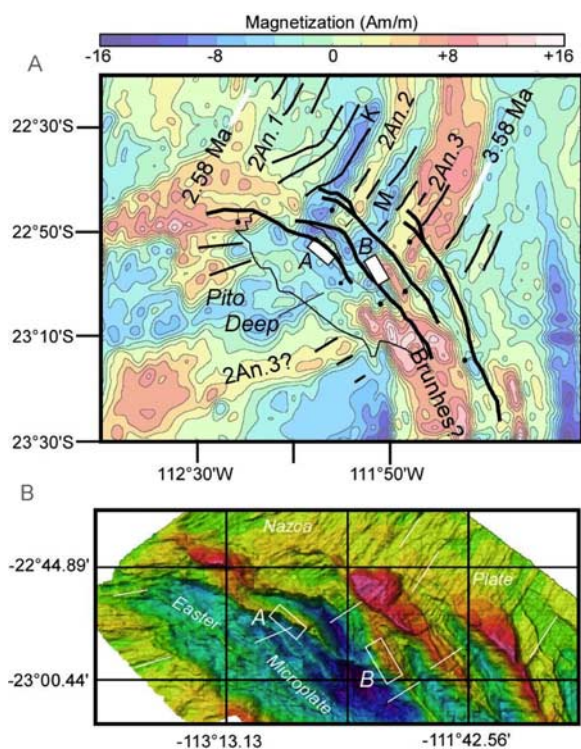


Figure 2. (a) Map of the northeastern Easter microplate and surrounding Nazca plate region. Color contours show the magnetization solution from inversion of sea surface magnetic anomaly data and bathymetry (incorporating data used by Martinez *et al.* [1991] and more recent data of Karson *et al.* (unpublished cruise report, 2005)). A magnetic source layer 1 km thick was assumed, and the solution was determined using a band-pass filter which passes wavelengths of 100 to 7 km unattenuated and removes wavelengths >200 km or <3.5 km. Heavy lines indicate probable main normal faults (barbell on downthrown side) bounding the northeast edge of the Pito Deep Rift (enclosed area > ~4200 m depth labeled “Pito Deep”). Fine lines show prominent bathymetric lineaments interpreted from detailed SeaBeam data [Karson *et al.*, 2005] presumed to parallel faults and fissures. White boxes show detailed study areas “A” and “B” of the 2005 Pito Deep cruise [Karson *et al.*, 2005]. Note near-parallelism of bathymetric lineaments and crustal magnetization and the continuation of positive magnetization into both study areas. Magnetization trends northeast of study areas are continuous with those of the Nazca plate (ages of beginning and end of anomaly 2A [from Cande and Kent, 1995] shown; K, Keana; M, Mammoth reversals, respectively), while more east-west trends southwest of the Pito Deep Rift are in crust of the Easter microplate. Northwest trending, possibly Brunhes, magnetization is inferred to be related to recent eastern propagator. Anomaly identification after Rusby and Searle [1995] and Martinez *et al.* [1991]. (b) Detailed SeaBeam data showing topographic lineaments in dive areas (A, B) and surrounding region. Thin, white lines are parallel to local lineaments. Note that lineaments vary from northeast to east-northeast trending across the transition from Nazca plate crust to the Easter microplate. Data from D. Naar cited by Karson *et al.* (unpublished cruise report, 2005). Bathymetry varies from ~6000 m (dark blue) to ~2000 m (red).

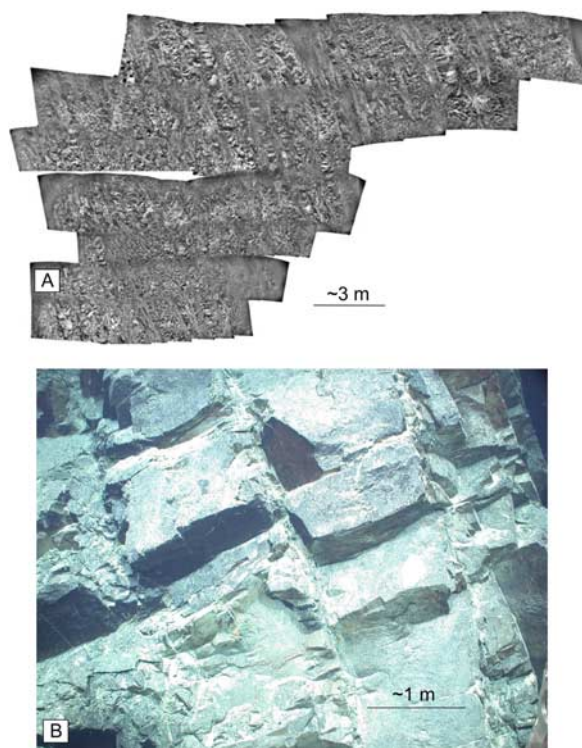


Figure 3. (a) Photographic mosaic of well-exposed, steeply southeast dipping sheeted dikes at ~ 3213 m depth along Jason II transect 5 (Karson et al., unpublished cruise report, 2005). Dikes in this area average ~ 1 m in width. View to northeast. Mosaicking by Steve Hurst. (b) Close-up photograph of southeast dipping dikes taken at ~ 3084 m depth during Alvin dive 4081. View is to northeast. Note well-developed, dike-parallel fractures that dip steeply to right (southeast) and dike-perpendicular cooling fractures dipping shallowly to left.

[5] Dikes averaging 1–2 m in thickness are beautifully exposed in each of the two study areas (Figure 3). The orientation of dikes is visually obvious in most localities with a dominant pattern of continuous fractures parallel to the dike margins and an orthogonal set of discontinuous fractures representing cooling joints. This interpretation is confirmed in many cases by observation of dike chilled margins in oriented samples. We were able to use the Geocompass to measure dike orientations directly. With only a few exceptions, the dikes dip southeast and strike northeast (Figure 4), subparallel to the orientation of bathymetric lineaments and magnetic anomaly directions in adjacent Nazca plate crust immediately to the northeast (Figure 2).

[6] To interpret flow directions in dikes exposed at the Pito Deep Rift it is critical to restore them to

their original orientation when they were formed at the EPR. To accomplish this, we compare the characteristic remanent magnetization (ChRM; determined from stepwise thermal or alternating field demagnetization) of dikes to the expected time-averaged magnetic direction at the site (000° – -40° for normal polarity). Because the remanence of an individual dike may also reflect paleosecular variation of the magnetic field, we collected samples from 11 subparallel dikes in a relatively small area (Alvin dive 4081; Figure 3b) to allow calculation of an average remanence direction that should minimize effects of paleosecular variation. Any remaining differences with respect to the expected direction should reflect structural rotations.

[7] ChRM in cores from oriented blocks was interpreted from principal component analysis of demagnetization data [Kirschvink, 1980]. Median destructive temperature (temperature at loss of 50% NRM) averages $\sim 520^\circ\text{C}$ and susceptibility of standard (2.54 cm diameter, 2.16 cm length) cores averages $\sim 6000 \mu\text{SI}$, both suggesting probable dominance of low-Ti titanomagnetite as the principal carrier of magnetic remanence as well as the dominance of ferromagnetic contributors to AMS fabrics.

[8] ChRM data from 10 of 11 dikes from Alvin dive 4081 that gave reliable results are shown in Figure 4a. The data are normal polarity (up to the north for the southern hemisphere), and have a dispersion that suggests that these data approximately average out paleosecular variation. The site mean is well removed from the expected position suggesting that significant, post-intrusion structural rotations have occurred. Significantly, this subset of data from closely spaced sampling in a small area also suggest relatively small errors related to Geocompass measurement, to sampling or to post-dive reorientation.

[9] ChRM directions from all 36 oriented blocks are shown in reference to the current, expected direction for the Pito Deep Rift (Figure 4d). Directions are dominantly normal as predicted from the location of the two study areas adjacent to areas of positive crustal magnetization (Figure 2). Despite consideration of secular variation ($\sim 14^\circ$) [McElhinny and McFadden, 1997] and probable measurement errors ($\sim 10^\circ$) [Cogné et al., 1995; Varga et al., 2004], the average remanence direction is well removed from the expected directions, again indicating post-intrusion structural rotations.

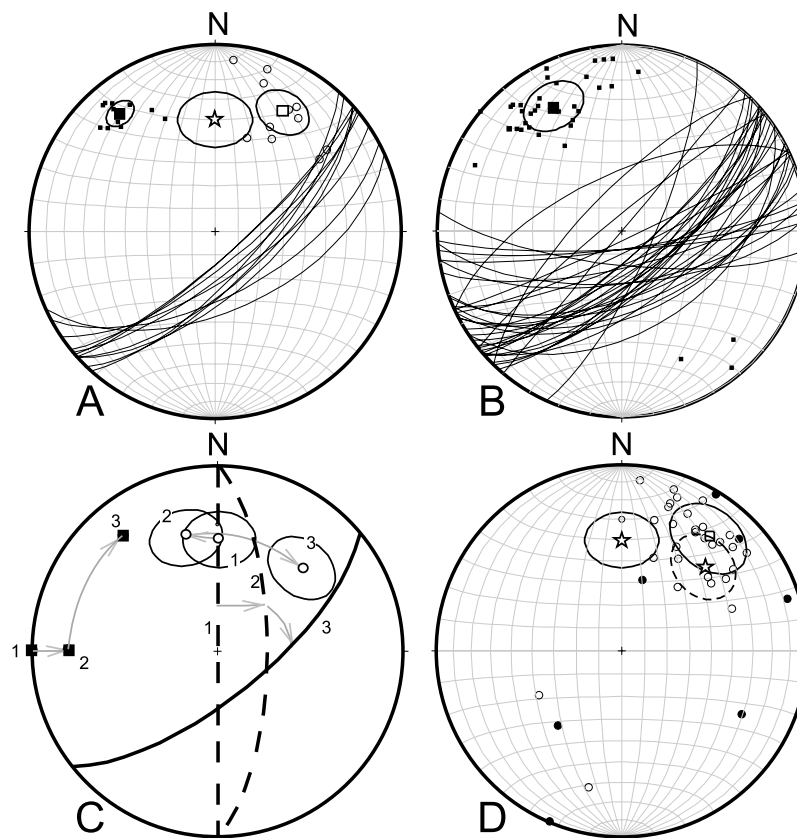


Figure 4. Stereographic projections (all equal-area) of field and magnetic remanence data. Great circles (dike margins) are plotted into lower hemisphere. Open symbols are plotted in upper hemisphere, and closed symbols are plotted in the lower hemisphere. (a) Data from Alvin dive 4081. Star is expected normal north direction (up to the north for southern hemisphere) at Pito Deep ($000^{\circ}/-40^{\circ}$) surrounded by a 14° small circle representing approximate expected secular variation [McElhinny and McFadden, 1997]. Open square is Fisher-distributed vector mean ($030^{\circ}/-27^{\circ}$) of ChRM (open circles) directions for 11 blocks of oriented dikes surrounded by its α_{95} confidence interval. Small closed square symbols are poles to dike margins, and large closed square is vector mean to dike poles surrounded by its α_{95} confidence ellipse. (b) Field data associated with 36 oriented blocks collected from both study areas A and B (Figure 2). Dike margin orientations (great circles) and their poles (small closed squares). Large closed square and its α_{95} error ellipse represent vector mean pole to average dike margin ($061^{\circ}/66^{\circ}$). (c) Two-stage rotation model. Vertical dikes produced at EPR (dashed great circle 1) rotated through normal faulting by $\sim 24^{\circ}$ (dashed great circle 2) about strike of dikes which rotates dike remanence (open circles and surrounding 14° small circles representing secular variation) from position 1 to 2. Clockwise rotation of Easter microplate causes subsequent 61° vertical axis rotation of dikes and remanence to current positions 3. Closed square symbols show pole to dikes at each stage. (d) ChRM data for 36 oriented blocks. Each open (upper hemisphere) or closed (lower hemisphere) circle represents a block-averaged site mean. Open star surrounded by solid confidence ellipse as in Figure 4a. Open star surrounded by dashed confidence ellipse represents expected remanence direction after two-stage rotation model discussed above (Figure 4c). Open square and ellipsoid confidence intervals as in Figure 4a.

[10] There is no unique number or path of structural rotations determined simply by the current orientation of dikes at the Pito Deep Rift. However, we can compare our data to a sequence of model rotations that represent a likely sequence of geological events for the area, a methodology that has been successful in restoring rotated dikes in both oceanic crust and in ophiolites [Varga, 2003; Varga

et al., 1999, 2004]. Our model invokes an initial rotation at the spreading center of $\sim 24^{\circ}$ about a ridge-parallel, horizontal axis that would produce the observed southeast dip of dikes. This interpretation is based on the assumption that the average dike orientation was approximately vertical when formed and that tilting beneath the ridge axis results from rotation of blocks bounded by normal

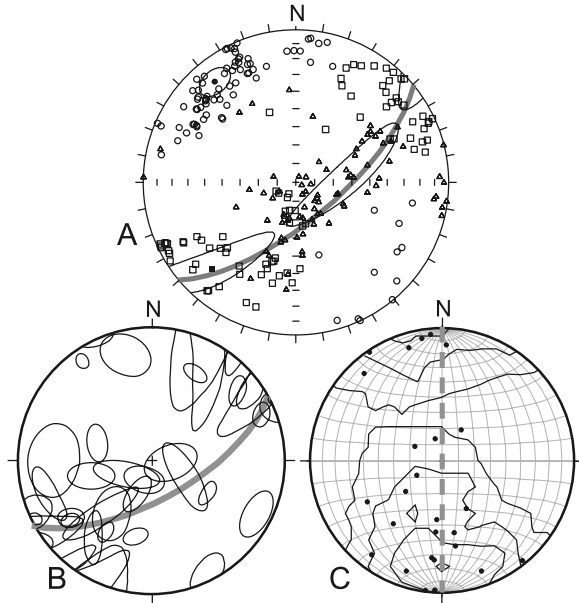


Figure 5. Stereographic projections (all equal-area) of AMS data from all oriented blocks. All data plotted into the lower hemisphere. (a) AMS ellipsoid k_1 (open squares), k_2 (open triangles), k_3 (open circles) axes, bootstrapped means (corresponding closed symbols), and confidence intervals (ellipses) for all oriented dike blocks from Alvin dive 4081. Each symbol represents measurement of a single core sample. Thick great circle is average dike orientation ($051^\circ/69^\circ$). All data plotted into the lower hemisphere. (b) The k_1 confidence ellipses for all oriented blocks with distinct k_1 orientations. Thick great circle is average dike orientation from data in Figure 5a. (c) The k_1 directions for 26 oriented blocks displaying “normal” symmetry with respect to dike margins. Contours are in intervals of 2σ from an assumed random distribution. Data have been returned to their assumed, original “EPR” coordinates using the two-stage rotation model discussed in text and in Figure 4c. Dashed great circle represents vertical dike.

faults. This kinematic pattern appears to be an important mode of deformation in the upper oceanic crust formed at fast spreading ridges that is exposed in tectonic windows and sampled by deep crustal drilling [Karson, 2002]. This interpretation is compatible with our observation of fault-related breccias bounding panels of southeast dipping dikes (J. A. Karson et al., unpublished cruise report, 2005). These dike-parallel breccias are similar to those observed in ophiolites where the crust is inferred to have been structurally extended by rotational-planar, dike-parallel normal faults near the ridge axis [Varga, 1991, 2003]. Our model invokes a second, vertical axis, clockwise rotation of 61° to explain the northeast strike of the dikes.

This rotation is related to rotation of the Easter microplate which, apparently, was coupled to Nazca plate crust to the north. This second rotation explains the northeast strike of dikes at the Pito Deep Rift and the northeast trend of dike ChRM directions that are clearly displaced in a clockwise direction from their expected orientation when formed.

[11] Figure 4c illustrates the two step rotation model and shows the path of both dike and ChRM orientations to their final positions. Note that our ChRM data from the Pito Deep Rift dikes (Figure 4d) is generally compatible with the model. Indeed the two-step model explains both the northeast trend of ChRM as well as the *apparent* greater rotation of dikes than corresponding ChRM orientations (Figures 4a and 5b). In detail, however, the ChRM mean is slightly shallower and has a more northerly trend than the model. This difference may reflect slight errors in the model assumptions about the original strike of dikes at the ridge axis and $\sim 10^\circ$ north-directed tilt in crustal blocks bounded by NW striking normal faults bounding the Pito Deep Rift (Figure 2), respectively. We note that our model does predict an angular divergence between the north/south trend of the EPR and the ChRM of tilted dikes near the ridge axis. This divergence is a testable prediction of our restoration and, if generally applicable, might represent a theoretically observable skewness to magnetic anomalies at the EPR.

[12] The AMS of 314 cores from oriented blocks was determined on an AGICO Kappabridge KLY 2. AMS fabric is characterized by a second-rank tensor commonly depicted by a representation ellipsoid with eigenvectors k_1 , k_2 , k_3 and corresponding eigenvalues $K_1 \geq K_2 \geq K_3$. The degree of anisotropy ($100 * (K_1 - K_3)$) [Tauxe, 2002] ranges between 0.07% and 3.4% with a mean anisotropy of 0.6%, similar to that found in studies of dikes in ophiolites [Rochette et al., 1991; Staudigel et al., 1999]. Representation AMS ellipsoids are highly prolate to triaxial (e.g., $K_1 > K_2 \geq K_3$).

[13] Figure 5a shows typical AMS data from Pito Deep Rift dikes. In this diagram we have plotted all of the individual core data from the 11 subparallel dikes collected on Alvin dive 4081. The mean positions for k_1 (squares), k_2 (triangles) and k_3 (circles) and their confidence ellipses were calculated using bootstrap statistics [Constable and Tauxe, 1990]. The symmetry of these AMS data with respect to the dike margin orientation is

typical of that found in most Pito Deep Rift dikes. Note that mean k_1 and k_2 lie close to the average dike margin in this area while k_3 lies at a high angle to the margin. There is also clear distinction between the eigenvectors as shown by lack of overlap of their respective confidence ellipses. Detailed study of such “normal” fabrics in mafic dikes from a variety of geologic settings indicates that k_1 directions are close to magmatic flow directions determined independently by field and microscopic criteria [Knight and Walker, 1988; Shelley, 1985; Tauxe et al., 1998; Varga et al., 1998]. These studies support a model in which AMS is controlled by late-crystallizing magnetic carriers (typically titanomagnetite in mafic dikes) that fill interstitial spaces between a flow-aligned silicate (typically plagioclase) fabric [Hargraves et al., 1991]. AMS data from Alvin dive 4081 dikes would thus be interpreted as indicating near-horizontal flow of magma during emplacement.

[14] To summarize AMS data from Pito Deep, we have plotted (Figure 5b) the confidence intervals surrounding k_1 axes for 30 of the samples that gave interpretable results and where k_1 is distinct from the other axes (k_2 , k_3). Note that 26 of the 30 blocks that meet this criteria have normal fabrics while four samples have so-called “inverse” fabrics where k_1 lies at a high angle to the average dike margin [Tauxe, 2002]. Of the samples with normal fabrics, 5 have relatively steep k_1 axes while the majority have shallow to moderately inclined k_1 axes. Figure 5c shows these k_1 data plotted in “EPR coordinates” after restoring dikes to their ridge crest orientation of formation using the above, two-step rotational model (Figure 4c). Interpreting k_1 in these normal fabrics as indicative of the magmatic flow direction, magma transport in Pito Deep Rift dikes was predominantly near-horizontal and parallel to the EPR.

[15] Shallow intrusive directions are particularly surprising because original magma flow direction is typically best recorded within <10 cm of chilled dike margins and these margins were generally not visible during seafloor outcrop sampling. Dikes commonly show steeper flow fabrics in their interiors due to drain-back during the waning phase of flow when magmatic fluid pressures drop. Thus, our sample collection might be expected to include many dike interiors where magma is subject to vertical, gravitational drain-back which can overprint earlier fabrics. The four inverse fabrics are difficult to explain in terms of magma flow. Such fabrics have been interpreted as being due to a

variety of causes including “rolling” of elongate grains during fluid flow, alteration, magnetic grain size, and dike width [Rochette et al., 1991, 1999].

[16] In summary, a majority of AMS fabrics in dikes from two study areas of the Pito Deep Rift indicate near-horizontal magma flow at the EPR ridge crest ~3 Ma ago. These results highlight the importance of lateral melt migration from localized magma chambers as a means of distributing magma along spreading center segments. They support inferences based on the geochemistry of dikes and lavas in tectonic windows from intermediate to superfast spread crust wherein the upper crust is constructed from dikes and lavas derived from magma sources that developed at different locations along the ridge axis [Pollock et al., 2005; Stewart et al., 2002]. Though we cannot uniquely determine the *sense* of magma flow in this study, the southern plunge of the majority of k_1 directions (Figure 5c) may suggest upward flow to the north, possibly toward a segment boundary and away from a centralized magma chamber. These results document lateral magma migration at a superfast spreading center, suggesting that such migration occurs even beneath ridges with evidence for nearly continuous subaxial magma chambers. Our data also demonstrate the utility of the AMS method for study of igneous flow patterns in modern ocean crust and the feasibility of collecting fully oriented blocks using ROVs which allows nearly continuous sampling over long time periods and in difficult terrain.

Acknowledgments

[17] We thank the crew, support staff, and scientific participants of Atlantis cruise AT11–23. This research was supported by National Science Foundation awards OCE 0222154 and OCE 0221948 and The College of Wooster.

References

- Allerton, S., and M. A. Tivey (2001), Magnetic polarity structure of the lower oceanic crust, *Geophys. Res. Lett.*, *28*, 423–426.
- Baragar, W. R. A., et al. (1987), Sheeted dikes of the Troodos ophiolite, Cyprus, in *Mafic Dyke Swarms*, edited by H. C. Halls and W. F. Fahrig, pp. 257–272, Geol. Assoc. of Can., Vancouver, Canada.
- Cann, J. R. (1970), New model for the structure of ocean crust, *Nature*, *226*, 928–930, doi:10.1038/226928a0.
- Cogné, J. P., et al. (1995), Large rotation of Easter microplate as evidenced by oriented paleomagnetic samples from the ocean floor, *Earth Planet. Sci. Lett.*, *136*, 213–222, doi:10.1016/0012-821X(95)00191-E.
- Constable, C., and L. Tauxe (1990), The bootstrap for magnetic susceptibility tensors, *J. Geophys. Res.*, *95*, 8383–8395, doi:10.1029/JB095iB06p08383.



- Delaney, J. R., et al. (1998), The quantum event of oceanic crustal accretion: Impacts of diking at mid-ocean ridges, *Science*, *281*, 222–230, doi:10.1126/science.281.5374.222.
- Dunn, R. A., and D. R. Toomey (1997), Seismological evidence for three-dimensional melt migration beneath the East Pacific Rise, *Nature*, *388*, 259–262, doi:10.1038/40831.
- Francheteau, J., et al. (1994), Submersible observations of the Easter microplate and its boundary, *Eos Trans. AGU*, *75*, 582.
- Hargraves, R. B., et al. (1991), Distribution anisotropy: The cause of AMS in igneous rocks?, *Geophys. Res. Lett.*, *18*, 2193–2196, doi:10.1029/91GL01777.
- Hurst, S., et al. (1994), Paleomagnetism of tilted diked in fast spread oceanic crust exposed in the Hess Deep Rift: Implications for spreading and rift propagation, *Tectonics*, *13*, 789–802, doi:10.1029/94TC00845.
- Karson, J. A. (1998), Internal structure of oceanic lithosphere: A perspective from tectonic windows, in *Faulting and Magmatism at Mid-Ocean Ridges*, *Geophys. Monogr. Ser.*, vol. 106, edited by W. R. Buck et al., pp. 177–218, AGU, Washington, D. C.
- Karson, J. A. (2002), Geologic structure of uppermost oceanic crust created at fast- to intermediate-rate spreading centers, *Annu. Rev. Earth Planet. Sci.*, *30*, 347–384, doi:10.1146/annurev.earth.30.091201.141132.
- Karson, J. A., et al. (2005), Nested-scale investigation of tectonic widows into super-fast spread crust exposed at the Pito Deep rift, Easter microplate, SE Pacific, *InterRidge News*, *14*, 5–8.
- Kirschvink, J. L. (1980), The least-squares line and plane and the analysis of palaeomagnetic data, *Geophys. J. R. Astron. Soc.*, *62*, 699–718.
- Knight, M. D., and G. P. L. Walker (1988), Magma flow directions in dikes of the Koolau Complex, Oahu, determined from magnetic fabric studies, *J. Geophys. Res.*, *93*, 4301–4320, doi:10.1029/JB093iB05p04301.
- Macdonald, K. C., et al. (1988), A new view of the mid-ocean ridge from the behavior of ridge-axis discontinuities, *Nature*, *335*, 217–225, doi:10.1038/335217a0.
- MacDonald, W. D., and H. C. Palmer (1990), Flow directions in ash-flow tuffs: A comparison of geological and magnetic susceptibility measurements, Tshirege member (upper Bandelier Tuff), Valles caldera, New Mexico, USA, *Bull. Volcanol.*, *53*, 45–59, doi:10.1007/BF00680319.
- Martinez, F., et al. (1991), Three-dimensional SeaMARC II, gravity, and magnetics study of large-offset rift propagation at the Pito rift, Easter microplate, *Mar. Geophys. Res.*, *13*, 255–285, doi:10.1007/BF00366279.
- McElhinny, M., and P. McFadden (1997), Paleosecular variation over the past 5 Myr based on a new generalized database, *Geophys. J. Int.*, *131*, 240–252, doi:10.1111/j.1365-246X.1997.tb01219.x.
- Naar, D. F., and R. N. Hey (1991), Tectonic evolution of the Easter microplate, *J. Geophys. Res.*, *96*, 7961–7993, doi:10.1029/90JB02398.
- Pollock, M., et al. (2005), Geochemical variability of dikes and lavas exposed in the Pito Deep, *Eos Trans. AGU*, *86*(52), Fall Meet. Suppl., Abstract T33D-0585.
- Rochette, P., et al. (1991), Diabase dike emplacement in the Oman ophiolite: A magnetic fabric study with reference to geochemistry, in *Ophiolite Genesis and Evolution of the Oceanic Lithosphere*, edited by T. Peters and R. G. Coleman, pp. 55–82, Kluwer Acad., Norwell, Mass.
- Rochette, P., et al. (1999), Is this magnetic fabric normal? A review and case study in volcanic formations, *Tectonophysics*, *307*, 219–234, doi:10.1016/S0040-1951(99)00127-4.
- Rusby, R. I., and R. Searle (1995), A history of the Easter microplate, 5.25 Ma to present, *J. Geophys. Res.*, *100*, 12,617–12,640, doi:10.1029/94JB02779.
- Searle, R. C., et al. (1989), Comprehensive sonar imaging of the Easter microplate, *Nature*, *341*, 701–705, doi:10.1038/341701a0.
- Shelley, D., et al. (1985), Determining paleo-flow directions from groundmass fabrics in the Littleton radial dykes, New Zealand, *J. Volcanol. Geotherm. Res.*, *25*, 69–79, doi:10.1016/0377-0273(85)90005-8.
- Sigurdsson, H., and S. R. J. Sparks (1978), Lateral magma flow within rifted Icelandic crust, *Nature*, *274*, 126–130, doi:10.1038/274126a0.
- Staudigel, H., et al. (1999), Geochemistry and Intrusive Directions in Sheeted Dikes in the Troodos Ophiolite: Implications for Mid-Ocean Ridge Spreading Centers, *Geochem. Geophys. Geosyst.*, *1*(1), 1001, doi:10.1029/1999GC000001.
- Stewart, M. A., E. M. Klein, and J. A. Karson (2002), Geochemistry of dikes and lavas from the north wall of the Hess Deep Rift: Insights into the four-dimensional character of crustal construction at fast spreading mid-ocean ridges, *J. Geophys. Res.*, *107*(B10), 2238, doi:10.1029/2001JB000545.
- Tauxe, L. (2002), *Paleomagnetic Principals and Practice*, 300 pp., Springer, Dordrecht, Netherlands.
- Tauxe, L., et al. (1998), Flow directions in dikes from anisotropy of magnetic susceptibility data: The bootstrap way, *J. Geophys. Res.*, *103*, 17,775–17,790, doi:10.1029/98JB01077.
- Varga, R. J. (1991), Modes of extension at oceanic spreading centers: Evidence from the Solea graben, Troodos ophiolite, Cyprus, *J. Struct. Geol.*, *13*, 517–537, doi:10.1016/0191-8141(91)90041-G.
- Varga, R. J. (2003), The sheeted dike complex of the Troodos ophiolite and its role in understanding mid-ocean ridge processes, in *Ophiolite Concept and the Evolution of Geological Thought*, edited by Y. Dilek and S. Newcomb, *Spec. Pap. Geol. Soc. Am.*, *373*, 323–336.
- Varga, R. J., et al. (1998), Dike surface lineations as magma flow indicators within the sheeted dike complex of the Troodos ophiolite, Cyprus, *J. Geophys. Res.*, *103*, 5241–5256, doi:10.1029/97JB02717.
- Varga, R. J., et al. (1999), Early establishment of seafloor hydrothermal systems during structural extension: Paleomagnetic evidence from the Troodos ophiolite, Cyprus, *Earth Planet. Sci. Lett.*, *171*, 221–235, doi:10.1016/S0012-821X(99)00147-8.
- Varga, R. J., et al. (2004), Paleomagnetic constraints on deformation models for uppermost oceanic crust exposed at the Hess Deep rift: Implications for axial processes at the East Pacific Rise, *J. Geophys. Res.*, *109*, B02104, doi:10.1029/2003JB002486.
- White, S. M., et al. (2000), Basaltic lava domes, lava lakes, and volcanic segmentation the southern East Pacific Rise, *J. Geophys. Res.*, *105*, 23,519–23,536, doi:10.1029/2000JB900248.